Leibniz-Gemeinschaft

Abschließender Sachbericht

Mathematische Modelle für Phasenübergänge in Lithium-Ionen-Batterien

Leibniz-Einrichtung:	Weierstraß-Institut für Angewandte Analysis und Stochastik
Aktenzeichen:	SAW-2012-WIAS-1 182
Projektlaufzeit:	01.07.2012 - 30.06.2015
Ansprechpartner:	Prof. Dr. Wolfgang Dreyer

Inhaltsverzeichnis

1 Executive summary

Innerhalb des Leibniz-Vorhabens *Mathematische Modelle für Phasenübergänge in Lithium-Ionen-Batterien* wurden substantielle Beiträge zu den folgenden Komponenten einer Lithium-Ionen-Batterie erarbeitet:

Vielteilchenkathode. Das anfängliche Modell zur Beschreibung des Lade/Entlade-Prozesses ging von einem Ensemble gleicher Speicherteilchen aus. In einer realen Vielteilchenkathode liegt aber eine Größenverteilung der Teilchen vor. Für relevante Voraussagen muss diese Größenverteilung modelliert werden, was aber im Fokker-Planck-Modell zu großen Schwierigkeiten führt. Dieses Modell wurde deshalb durch ein äquivalentes, aber viel einfacher zu handhabendes stochastisches Modell ersetzt. Simulationen zeigen, dass die Teilchenverteilungen, insbesondere beim schnellen Laden/Entladen, einen wesentlichen Einfluss auf die Spannungs-Kapazitäts-Kurve der Vielteilchenkathode hat. Es existieren optimale und weniger nützliche Teilchengrößenverteilungen.

Elektrolyt. Die Modellierung einer elektrolytischen Lösung war ursprünglich nicht geplant. Es stellte sich aber heraus, dass für eine Bewertung des experimentellen Verhaltens der Vielteilchenelektrode deren Kopplung an den Elektrolyt essentiell ist. Da die vorhandenen Elektrolytmodelle in diesem Zusammenhang völlig ungeeignet sind, wurde im Rahmen des Leibniz-Vorhabens ein neues Elektrolytmodell aufgestellt. Insbesondere dieses Modell hat international zu einer großen Sichtbarkeit der Leibniz-Gruppe geführt. Die wesentlichen Neuerungen betreffen (i) die erstmalige Berücksichtigung der Wechselwirkung von Lösungsmittel und Ionen, (ii) die in der Elektrochemie unbekannte Kopplung der Diffusionsgleichungen mit der Impulsbilanz, und (iii) die Beschreibung der Solvatisierung der Ionen in einem thermodynamisch konsistenten Modell.

Elektrolyt/Elektrode Grenzfläche. Die entscheidenden Prozesse einer Batterie laufen auf der Grenzfläche zwischen Elektrode und Elektrolyt ab. Auf der Grenzfläche zwischen der Vielteilchenkathode und dem Elektrolyt sind dies die Adsorption von Lithium-Ionen und Lithium-Atomen und die Elektrontransferreaktionen. Auch hier ist die relevante Modellierung im Leibniz-Vorhaben durchgeführt worden. Die Herausforderung bestand hier in der Kopplung von Thermo- und Elektrodynamik für Flächen und bei der Herleitung von Materialgleichungen. Die neuen Modelle für die Elektrolyt/Elektroden Grenzfläche vermögen erstmalig die Struktur der Raumladungszonen an der Grenzfläche richtig zu beschreiben. Insbesondere konnten erstmalig Grenzflächenkapazitäten für unterschiedliche Metall/Elektrolyt Systeme wiedergeben werden, die qualitativ und quantitativ in Übereinstimmung mit Messdaten sind.

Die asymptotische Analysis der Grenzfläche und ihrer wenige Nanometer breiten Randschichten liefert reduzierte Modelle, welche eine neue Interpretation bekannter Modelle der Elektrochemie erlaubt. Dadurch wird eine Behebung der Defizite der klassischen Gleichungen möglich.

Glanzlichter. Sowohl die Vorarbeiten als auch die während des Bestehens der Leibniz-Gruppe veröffentlichten Resultate haben zu einer großen Sichtbarkeit geführt. Belegt wird dies durch ungefähr 300 Zitate, die sich auf die diversen Veröffentlichungen in wichtigen Journalen der Elektrochemie beziehen. Darüber hinaus hat es etwa 40 eingeladene Vorträge gegeben, darunter einige mit populärem Charakter. Während der Laufzeit des Projektes wurde die ursprüngliche Antragsidee experimentell bestätigt. Im Zusammenhang mit dem Leibniz-Projekt hat Clemens Guhlke 2014 an der TU Berlin die mit *Summa Cum Laude* bewertete Dissertation zur Theorie der elektrochemischen Grenzfläche vollendet. Diese Arbeit wird die Elektrochemie in den nächsten Jahren entscheidend beeinflussen.

2 Projektbeschreibung

Nach dem *nationalen Entwicklungsplan Elektromobilität* der Bundesregierung sollen bis 2020 mehr als eine Million Elektrofahrzeuge auf Deutschlands Straßen fahren. Um dieses ehrgeizige Ziel zu erreichen, werden neue Batteriematerialien für Lithium-Ionen-Batterien entwickelt und optimiert. Hierbei spielen das Verständnis der elektrochemischen und physikalischen Prozesse innerhalb der Batterie und deren mathematische Beschreibung eine zentrale Rolle. Dies ist der zentrale Gegenstand des Vorhabens *Mathematische Modelle für Phasenübergänge in Lithium-Ionen-Batterien*.

Das Funktionsprinzip einer Lithium-Ionen-Batterie beruht auf dem System Anode-Kathode-Elektrolyt. Die Abbildung 1_{links} zeigt eine vereinfachte Darstellung und die Funktionsweise einer Lithium-Ionen Batterie.

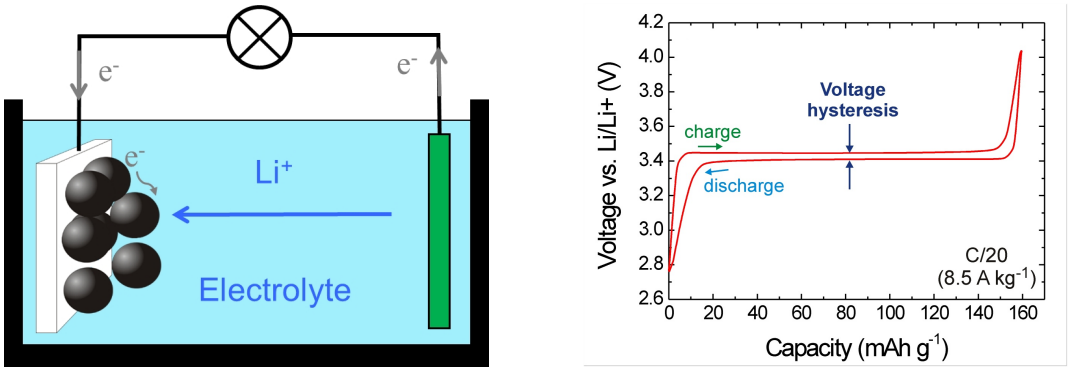

Abbildung 1: links: Darstellung Aufbau und Funktionsweise einer Lithium-Ionen-Batterie, rechts: Spannungs-Kapazitäts-Verlauf einer $LiFePO_4$ Batterie, [1].

Die Zielsetzung des Vorhabens lag bei der mathematischen Modellierung und der Untersuchung von Batterieelektroden, die folgende zwei Eigenschaften besitzen: i) Das Elektrodenmaterial speichert Lithium in einem Vielteilchensystem, und ii) während des Ladens und Entladens der Batterie finden im Vielteichensystem Phasenübergänge statt.

Der Vielteilchencharakter der Elektrode führt dazu, dass zwei in Konkurrenz stehende Phasenübergänge auftreten. Ein Phasenübergang findet im Einzelteilchen statt, wohingegen ein zweiter Phasenübergang im Teilchenensemble auftritt. Die Phasenübergänge sind in der Abbildung 2 illustriert. Der Vielteilchenphasenübergang dominiert für langsames Laden das Verhalten der Batterie. Dies führt zu konstanten Spannungsplateaus und Hysterese im Spannungs-Kapazitäts-Diagramm, Abbildung 1_{rechts}. Der Phasenübergang im Einzelteilchen ist nur für schnelles Laden bzw. Entladen der Batterie innerhalb von Sekunden zu beobachten.

Die thermodynamische Modellierung, die Analyse und numerische Simulationen der Phasenübergänge in der Vielteilchenelektrode waren der zentrale Gegenstand dieses Vorhabens. Hierzu sollten die bereits bei Antragstellung vorhandenen Elektroden-Modelle durch Einbeziehung weiterer Phänomene ergänzt und analysiert werden. Die Ziele des Projekts zur Antragstellung waren im Einzelnen:

- Beschreibung des Phasenübergangs im Einzelteilchen mittels *Scharfer-Grenzschicht-Modelle* und *Phasenfeldmodelle* unter Berücksichtigung der Kristallsymmetrie des Speicherteilchens, welche zu anisotroper Diffusion und anisotropen Volumenspannungen führt.
- Erweiterung des *Vielteilchenmodells* auf das Schnell-Lade-Regime. Hierzu sollte der Phasenübergang im Teilchen mittels eines einfachen Core-Shell-Modells berücksichtigt werden.
- Beschreibung der *Nukleation* einer neuen Phase. Hierzu sollten das Vielteilchenmodell, welches Nukleation richtig beschreibt, mit dem Einteilchenmodell gekoppelt werden.

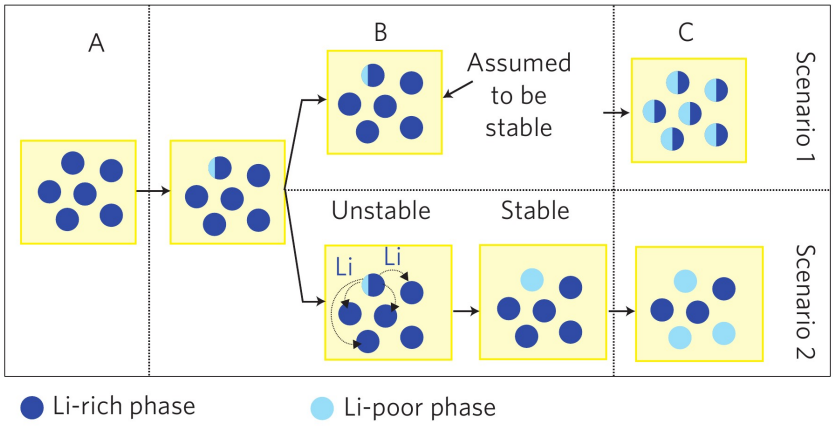

Abbildung 2: Mögliche Szenarien während des Füllens einer $LiFePO_4$ Vielteilchenelektrode, [1].

- Ein weiterer Schwerpunkt in diesem Vorhaben war der *mathematischen Analyse* der diversen Modelle gewidmet, insbesondere der Existenz, der Regularität und der Eindeutigkeit des Vielteilchenmodells. Ferner sind mit asymptotischen Methoden die scharfen Limites der diversen Phasenfeldversionen der Einteilchenmodelle durchzuführen.

Wir wollen nun auf die einzelnen Ziele, deren Umsetzung und auf neue Fragestellung eingehen.

Einteilchenmodelle. Bei der Modellierung des Phasenübergangs im Teilchen können zwei unterschiedliche Modellierungsansätze verfolgt werden. Zum einen kann der Phasenübergang mittels eines Scharfen-Grenzschicht-Modells beschrieben werden, andererseits mittels eines Phasenfeld-Modells. Beide Modelle besitzen Vor- und Nachteile. Die Scharfen-Grenzschicht-Modelle beschreiben die Phasengrenze als zweidimensionale Mannigfaltigkeit. Dies ermöglicht die Formulierung physikalischer Gesetze, die leicht experimentell verifizierbar sind. Anderseits muss für Computersimulationen die Bewegung der Phasengrenze mittels geeigneter numerischer Verfahren beschrieben werden. Dies entfällt bei Phasenfeld-Modellen, wo die Phasengrenze als eine Grenzschicht mit einer kontrollierbaren Dicke ε beschrieben wird. Die physikalischen Eigenschaften der Grenzschicht im Phasenfeld-Modell hängt stark vom gewählten Ansatz ab. Mittels einer Asymptotik für den Kleinheitsparameter ε können aus Phasenfeld-Modellen Scharfe-Grenzschicht-Modelle hergeleitet werden. Diese Scharfen-Grenzschicht-Modelle können leicht geprüft werden auf ihre thermodynamische Konsistenz.

Im Vorhaben sind Phasenfeld-Modelle für das Elektrodenmaterial Lithiumeisenphosphat hergeleitet worden. Diese Modelle berücksichtigen die elastischen Eigenschaften des Materials und die Eigenspannungen, die bei der Interkalation des Lithiums im Eisenphosphat auftreten. Für die Modellierung wurde der Lithiummolenbruch als natürliche Phasenfeldvariable verwendet. Dies führt auf Phasenfeld-Modelle vom Cahn-Hilliard-Typ. Bei der asymptotische Analyse der Phasenfeld-Modell zeigte sich aber, dass die resultierenden Scharfen-Grenzflächen-Modelle nicht thermodynamisch konsistent sind. Genauer, es konnte gezeigt werden, dass diese Modelle eine negative Flächenentropieproduktion aufweisen können. Weitere Untersuchungen zeigten, dass bereits die klassische Cahn-Hilliard Gleichung dieses Defizit besitzt. Im Fall der Cahn-Hilliard Gleichung konnte dieses Defizit mittels eine viskosen Regularisierung behoben werden, siehe [11]. Ob eine viskose Regularisierung die Defizite der Phasenfeld-Modelle mit Elastizität für das Lithiumeisenphosphat behebt, konnte noch nicht geklärt werden.

Unsere Untersuchungen zeigen, dass die Modellierung von Phasenübergängen im Einzelteilchen mittels Phasenfeld-Modellen kritisch zu bewerten ist und eine Untersuchung der physikalischen Eigenschaften des zugehörigen Scharfen-Grenzschicht-Modells unerlässlich ist.

Vielteilchenmodell. Zum Antragszeitpunkt wurde der Phasenübergang in der Vielteilchenelektrode mittels einer Fokker-Planck-Gleichung für langsames Laden/Entladen beschrieben. Ihre Herleitung basiert auf den folgenden Annahmen:

1. Homogene Teilchen, d.h. kein Phasenübergang im Einzelteilchen und keine Diffusionslimitierung in der Elektrode,
2. Unendliche Mobilität der Ionen im Elektrolyten,
3. Lokales Gleichgewicht für Adsorption der Lithiumionen vom Elektrolyten auf die Elektrodenoberfläche und lokales Gleichgewicht der Lithium-Interkalation in die Elektrode,
4. Unendlich schneller Elektronentransfer an der Elektrode-Elektrolyt-Grenzflächen,
5. Alle Elektrodenteilchen sind gleich groß,
6. Lithium kann auf der gesamten Elektrodenoberfläche interkalieren.

Zum Beginn des Vorhabens war die vorherrschende Meinung, dass der Phasenübergang im Einzelteilchen der limitierende Prozess beim schnellen Laden bzw. Entladen ist und das Verhalten der Batteriespannung wesentlich dominiert. Aktuelle experimentelle Untersuchungen der Arbeitsgruppe von W. Chueh zeigten aber, dass auch im Zeitregime von Minuten der Vielteilchenphasenübergang vorherrscht und nicht der Phasenübergang im Einzelteilchen [14, 15]. Wir schließen hieraus, dass beim schnellen Laden bzw. Entladen der Batterie die Annahme 1 erfüllt ist. Darüber hinaus zeigen die Arbeiten von Chueh et al., dass bei einem typischen Elektrodenabstand von 100μm die Diffusion im Elektrolyten sich im Gleichgewicht befindet und Annahme 2 gerechtfertig ist. Das Batterieverhalten für schnelles Laden muss also durch die Oberflächenprozesse bestimmt sein.

Die Teilchen in der Elektrode besitzen stark unterschiedliche Teilchengrößen, so dass auch dieser Aspekt bei der Modellierung nicht außer Acht gelassen werden darf. Abbildung 3 zeigt eine typische Teilchengrößenverteilung einer Vielteilchenelektrode. Im Vorhaben wurde deshalb neben der Interkalation, die Adsorption, die Elektronentransferreaktion und die Teilchengrößenverteilung ins Modell aufgenommen.

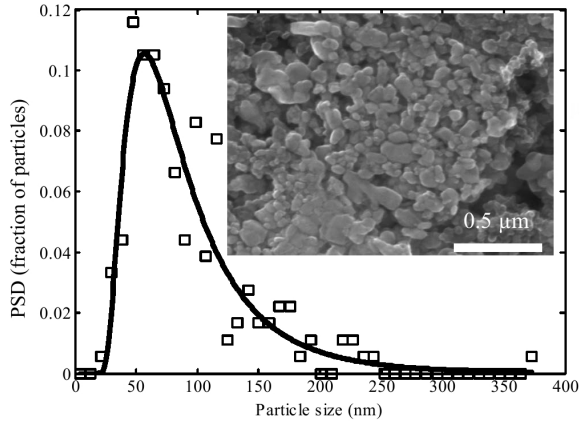

Abbildung 3: Teilchengrößenverteilung einer $LiFePO_4$ Vielteilchenelektrode aus [16]

Nukleation. Die Nukleation konnte zum Beginn des Vorhabens nur geeignet mittels der Fokker-Planck-Gleichung beschrieben werden. Sie basiert auf einer statistischen Beschreibung der Elektrode. Die Erweiterung der Fokker-Planck-Gleichung auf eine Teilchengrößenverteilung der Elektrodenteilchen ist sehr schwierig. Wohingegen die Berücksichtigung der Teilchengrößenverteilung im Kontext der Thermodynamik basierend auf den Massenbilanzgleichungen der

Einzelteilchen sehr einfach ist. Die Thermodynamik basiert auf deterministischen partiellen Differentialgleichungen. Eine thermodynamisch konsistente Modellierung von Fluktuationen, die die Nukleation einer neuen Phase hervorrufen, war bisher nicht bekannt. Im Zusammenhang mit der Vielteilchenelektrode konnte gezeigt werden, dass Fluktuationen im thermodynamische Setting modelliert werden können, d.h. universelle physikalische Gesetze wie Massen-, Impuls- und Energieerhalt in abgeschlossenen Systemen sind erfüllt und die Materialgleichungen erfüllen den zweiten Hauptsatz der Thermodynamik. Der neue Ansatz führt auf ein System stochastischer Differentialgleichungen (SDE). Angewendet auf die Vielteilchenelektrode und unter Berücksichtigung der obigen Annahmen 1-6 liefert das SDE-System für unendlich viele Teilchen die Fokker-Planck-Gleichungen [7]. Es ist uns gelungen, Nukleation auf der Ebene von Kontinuumsmodellen (Scharfe-Grenzschicht-Modelle und Phasenfeld-Modelle) zu modellieren und wir haben die Grundlagen geschaffen, Oberflächenphänomene in das Vielteilchenmodell mit aufzunehmen [7].

Neue Fragestellungen. Die Erweiterung des Vielteilchenmodells auf Adsorption und Elektronentransferreaktionen machte es notwendig die Prozesse an der Elektroden-Elektrolyt-Grenzfläche detaillierter zu beschreiben. Hierbei mussten wir jedoch feststellen, dass die vorhandenen Modelle für Grenzflächen in der Elektrochemie erhebliche Inkonsistenzen und Defizite besitzen! Diese sind begründet in folgenden Beobachtungen:

- Es existiert keine gesamtheitliche Betrachtungsweise, welche alle Phänomenen konsistent miteinanderkoppelt.
- Es wird nicht zwischen universellen und materialabhängigen Gleichungen unterschieden. Hierdurch ist die Übertragbarkeit auf andere (Batterie-) Systeme nur schwer oder gar nicht möglich.
- Es werden experimentelles Grundlagenwissen und Theoriebruchstücke zu neuen Modellen kombiniert, deren Parameter durch Fitten von Experimenten bestimmt werden.
- Es fehlt oft an exakten Definitionen, welche erst zu begrifflichen Ungenauigkeiten und dann zu Kontroversen führen.

Die Ursache dieser Defizite ist in der unterschiedlichen historischen Entwicklung von Elektrochemie und Thermodynamik zu finden.

Die Grundlage für eine rationale Kontinuumstheorie bildet die Thermodynamik. Sie wurde in den 1940er Jahren von Carl H. Eckart entwickelt, von Josef Meixner ausgebaut, und sie fand ihren vorläufigen Abschluss durch Sybren R. de Groot und Paul Mazur in der bedeutenden Monografie Non-equilibrium thermodynamics im Jahre 1963. Die Thermodynamik unterscheidet zwischen universellen und materialabhängigen Beziehungen, wobei die materialabhängigen Beziehungen unter anderem durch den zweiten Hauptsatz der Thermodynamik eingeschränkt werden.

Dagegen fand die mathematische Modellierung in der Elektrochemie bereits zum Ende des 19. Jahrhunderts durch Walter Nernst und Max Planck statt. Sie wurde dann recht schnell weiterentwickelt durch Peter Debye, Otto Stern, John A.V. Butler, Alexander Frumkin, Max Volmer und fand ihren theoretischen Abschluss durch David C. Grahame in den 1940er Jahren. Die in dieser Zeit entwickelten Modelle finden heute immer noch Anwendung in der Elektrochemie.

Die Resultate der Thermodynamik fanden deshalb nur wenig Berücksichtigung in der Elektrochemie oder wurden gänzlich ignoriert. In dem Vorhaben wurden deshalb, basierend auf der Thermodynamik, die mathematischen Modelle der Elektrochemie neu hergeleitet, diskutiert und wesentlich verbessert. Hierzu war zunächst die Erweiterung der Thermo- und Elektrodynamik auf elektrochemische Grenzflächen notwendig. Die neue Flächentheorie ist in der Dissertation [9] zusammengefasst.

3 Scientific highlights

3.1 Electrolyte model

The mathematical modeling of electrochemical phenomena, particularly in electrolytes, started already within the last ten years of the nineteenth century. In that time Walter Nernst and Max Planck laid down what nowadays is called Nernst-Planck model. Due to the missing non-equilibrium thermodynamics, the Nernst-Planck model exhibits some serious inherent deficiencies. However it is still often considered as the relevant theoretical basis and widely used.

We revisit the old Nernst-Planck model and removes its deficiencies by a rational thermodynamically consistent coupling between mechanics and diffusion. By the method of formal asymptotic expansion results for practical applications of the theory are derived. To keep this representation simple we do not consider temperature variations, polarization, viscosity and chemical reactions in detail and refer to [4, 8, 5, 6, 9].

Thermodynamic state of electrolytes. A liquid electrolyte is a chemically reacting mixture consisting of $N+1$ constituents $(A_\alpha)_{\alpha=0,1,...,N}$. Their particles have atomic masses $(m_\alpha)_{\alpha=0,1,2,...,N}$ and may be carrier of charges $(z_\alpha e_0)_{\alpha=0,1,2,...,N}$. The constant e_0 is the elementary charge and the z_α denote the charge number. The constituent with the index 0 is the neutral solvent, i.e. $z_0 = 0$.

At any time $t \geq 0$, the thermodynamic state of a mixtrue in a region $\Omega \subset \mathbb{R}^3$ is described by N particle densities $(n_\alpha)_{\alpha=0,1,2,...,N}$, the barycentric velocity $\boldsymbol{v}$ and the temperature T of the mixture and by the electric field $\boldsymbol{E}$. These quantities may be functions of time $t \geq 0$ and space $\boldsymbol{x}$.

Equations of balance for mass and momentum. The evolution of the thermodynamic state is determined by a coupled system of partial differential equations. Part of this system are the equations of balance for the $N + 1$ partial mass densities and for the barycentric momentum:

$$\partial_t m_\alpha n_\alpha + \operatorname{div}(m_\alpha n_\alpha \boldsymbol{v}_\alpha) = r_\alpha, \qquad \alpha = 0, 1, 2, ..., N \tag{1}$$

$$\partial_t \rho \boldsymbol{v} + \operatorname{div}(\rho \boldsymbol{v} \otimes \boldsymbol{v} - \boldsymbol{\sigma}) = \boldsymbol{k}\,. \tag{2}$$

Besides the variables from the last paragraph there occur new quantities here: $\boldsymbol{v}_\alpha$ - partial velocities, r_α - mass productions, $\boldsymbol{\sigma}$ - stress and $\boldsymbol{k}$ - Lorentz force density. These quantities must be related to the variables by constitutive equations. However, their generality is restricted because there are some important constraints. (i) The local conservation of total mass requires $\sum_{\alpha=0}^{N} r_\alpha = 0$. (ii) The barycentric velocities follow from the partial velocities by $\rho \boldsymbol{v} = \sum_{\alpha=0}^{N} m_\alpha n_\alpha \boldsymbol{v}_\alpha$ so that the mass density of the mixture, $\rho = \sum_{\alpha=0}^{N} m_\alpha n_\alpha$, satisfies the conservation law for total mass, $\partial_t \rho + \operatorname{div}(\rho \boldsymbol{v}) = 0$. (iii) The partial velocities are substituted by the diffusion fluxes, which are defined by $\boldsymbol{J}_\alpha = m_\alpha n_\alpha (\boldsymbol{v}_\alpha - \boldsymbol{v})$. Consequently, there are only $N - 1$ independent diffusion fluxes because we have the constraint $\sum_{\alpha=0}^{N} \boldsymbol{J}_\alpha = 0$. Thus the $N + 1$ partial mass balances split into the mass balance of the mixture and N diffusion equations,

$$\partial_t \rho + \operatorname{div}(\rho \boldsymbol{v}) = 0, \qquad \partial_t m_\alpha n_\alpha + \operatorname{div}(m_\alpha n_\alpha \boldsymbol{v} + \boldsymbol{J}_\alpha) = r_\alpha, \quad \alpha = 1, 2, ..., N\,. \tag{3}$$

The quasi-static setting of Maxwells equations. The full system of Maxwell's equation is considerably reduced if magnetic fields are ignored so that the electric field is given by a potential, $\boldsymbol{E} = -\nabla\varphi$. Then the equation determining the electric field is $\varepsilon_0 \operatorname{div}(\boldsymbol{E}) = n^{\mathrm{e}}$, where n^{e} is the electric charge density which, for simplicity, is represented here only by the density of free charges, $n^{\mathrm{e}} = n^{\mathrm{F}} = \sum_{\alpha=0}^{N} z_\alpha e_0 n_\alpha$. In this setting the Lorentz force in the momentum balance is simply given by $\boldsymbol{k} = -n^{\mathrm{F}} \nabla\varphi$.

Deficiencies of the Nernst-Planck model and their removal.

The essential flaws of the the Nernst-Planck model are

- local electro-neutrality in the whole electrolyte
- the pressure due to the constituents of the electrolyte is ignored
- the diffusion fluxes do not reflect the interaction of anions and cations with the solvent

To fully recognize the content of these assumptions let us consider more details.

Local electro-neutrality. Walther Nernst argues in his paper *Die elektromotorische Wirksamkeit der Ionen* from 1989 *...da im Innern der Lösungen keine freie Elektrizität (...) bestehen kann, so muss die Bedingung* $n^{\mathrm{F}} = 0$ *erfüllt sein.* Max Planck agrees with Nernst. One year later in *Über die Erregung von Electrizität und Wärme in Electrolyten* Planck gives an explanation by means of the Poisson equation which reads in dimensionless form

$$\lambda^2 \Delta\varphi = -n^{\mathrm{F}}. \tag{4}$$

Here λ is a small dimensionless parameter that defines a characteristic length scale $\lambda L^R = \sqrt{kT\varepsilon_0/e_0^2 n^{\mathrm{R}}}$. L^{R} may be the distance between two electrodes in the electrolyte and n^{R} is related to the overall density of the anions and cations. For $n^{\mathrm{R}} = 0.1$ mole per liter we have $\lambda L^{\mathrm{R}} = 1.5\ 10^{-10}$m which leads Planck to argue that (4) cannot be used to determine the potential φ. Moreover, he concludes that the only information attained from (4) is $n^{\mathrm{F}} = 0$. However, both statements are only true if $\Delta\varphi$ is of order $\mathcal{O}(1)$. In fact, this property is met in the bulk region of the electrolyte but not in the vicinity of the electrode-electrolyte interfaces where boundary layers develop with $\Delta\varphi = \mathcal{O}(1/\lambda^2)$. The extension of the model by using (4) instead of $n^{\mathrm{F}} = 0$ is called Poisson-Nernst-Planck model [4].

Coupling to mechanics. There is a further important law of nature that is ignored by Nernst and Planck and it is usually ignored even nowadays in electrochemistry. This is the conservation law of momentum. For simplicity of the illustration let us consider the equilibrium case and exclusively electric forces. Then the momentum balance reads

$$\nabla p = -n^{\mathrm{F}} \nabla\varphi, \tag{5}$$

where p denotes the local material pressure of the electrolyte. In the elastic case the pressure is given by a constitutive function of the form $p = \hat{p}(T, n_0, n_1, ...n_N, \boldsymbol{E})$. If the local charge neutrality (1) were satisfied everywhere, the pressure would be a constant in the whole electrolyte and equal to the outer pressure $p_0 \approx 1$ bar. However, in the vicinity of an electrode-electrolyte interface we have $n^{\mathrm{F}} \neq 0$. Combining (4) and (5) then yields

$$\mathrm{div}(\boldsymbol{\Sigma}) = 0 \quad \text{with} \quad \boldsymbol{\Sigma} = -\big(p + \tfrac{1}{2}\lambda^2 |\nabla\varphi|^2\big)\mathbf{1} + \lambda^2 \nabla\varphi \otimes \nabla\varphi. \tag{6}$$

The quantity $\boldsymbol{\Sigma}$ is the total stress of the electrolyte. Near to the boundary the gradients of the electric potential may become very large and this must be counterbalanced by the material pressure because at a boundary with normal $\boldsymbol{\nu}$, we obviously have $\boldsymbol{\Sigma} \cdot \boldsymbol{\nu} = -p_0 \boldsymbol{\nu}$.

Role of the solvent. The third wrong ingredient of the Nernst-Planck model is the ignorance of the solvent leading to a variety of subtle implications. These arise due to the special from of the N diffusion fluxes for the N dissolved constituents. The Nernst-Planck model proposes

$$\boldsymbol{J}_\alpha^{\mathrm{NP}} = -M_\alpha^{\mathrm{NP}} \Big(\nabla n_\alpha + \frac{z_\alpha e_0}{kT} n_\alpha \nabla\varphi \Big), \tag{7}$$

where $M_\alpha^{\mathrm{NP}} > 0$ are phenomenological coefficients. On the other hand, the general form of thermodynamically consistent diffusion fluxes are represented by,

$$\boldsymbol{J}_\alpha = -\sum_{\beta=1}^{N} M_{\alpha\beta}\left(\nabla\Big(\frac{\mu_\beta-\mu_0}{T}\Big)+\frac{1}{T}\Big(\frac{z_\beta e_0}{m_\beta}-\frac{z_0 e_0}{m_0}\Big)\nabla\varphi\right)\,. \tag{8}$$

The $M_{\alpha\beta}$ are the phenomenological coefficients of the symmetric and positive definite mobility matrix. The quantities μ_α are the chemical potentials. They are derivatives of the free energy density $\rho\psi$, which is the central constitutive quantity of continuum thermodynamics. In the present case we have $\psi = \hat{\psi}(T, n_0, n_1, ..., n_N, \boldsymbol{E})$. Then the chemical potentials are defined by $\mu_\alpha = \partial\rho\psi/\partial m_\alpha n_\alpha$. The appearance of the differences $\mu_\beta - \mu_0$ describes the interaction of the constituent A_β with the solvent A_0. These differences appear in the diffusion fluxes due to the constraint $\boldsymbol{J}_0 = -\sum_{\alpha=1}^{N}\boldsymbol{J}_\alpha$. For a comparison of the two diffusion laws we consider the most simple constitutive model for the electrolyte. It is the so called *incompressible simple mixture*, which Nernst and Planck presumably might had in mind when postulating their fluxes (7). With the constant reference values for the chemical potentials, μ_α^{R}, the pressure, p^{R}, and the partial molar volume, v_α^{R}, the chemical potentials for an incompressible simple mixture read

$$\mu_\alpha = \mu_\alpha^{\mathrm{R}} + \frac{v_\alpha^{\mathrm{R}}}{m_\alpha}(p-p^{\mathrm{R}}) + \frac{kT}{m_\alpha}\ln\Big(\frac{n_\alpha}{n}\Big) \qquad \text{with} \quad n=\sum_{\alpha=0}^{N} n_\alpha\,. \tag{9}$$

Now we ignore cross diffusion and assume that the diagonal mobilities are proportional to the particle densities, i.e. $M_{\alpha\alpha} = (k^{-1}m_\alpha M_\alpha^{\mathrm{NP}})n_\alpha$. Then the thermodynamically correct fluxes (8) are given by

$$\boldsymbol{J}_\alpha = -M_\alpha^{\mathrm{NP}}\left(\nabla n_\alpha + \frac{z_\alpha e_0}{kT}n_\alpha\nabla\varphi - \frac{m_\alpha n_\alpha}{m_0 n_0}\nabla n_0 + \frac{v_\alpha^{\mathrm{R}} n_\alpha}{kT}\Big(1-\frac{v_0^{\mathrm{R}}m_\alpha}{v_\alpha^{\mathrm{R}}m_0}\Big)\nabla p\right). \tag{10}$$

Hence only the first two terms of the correct fluxes agree with the Nernst-Planck fluxes (7) and the missing terms describe the ion-solvent interaction and the pressure contribution.

Implications of the extended model

In the following, four examples are given to illustrate the large importance of the missing phenomena in the Nernst-Planck model.

Pressure dependence of mole fractions. Between two electrodes with given potentials φ_{L} and φ_{R} we consider an electrolyte in equilibrium. Let the electrolyte consists of three constituents : positively charged cations C, negatively charged anions A, and the neutral solvent S. The corresponding mole fractions $y_\alpha = n_\alpha/n$ are y_{A}, y_{C} and y_{S}. The domain Ω can be decomposed into the boundary layers and the bulk part, where all quantities turn out to be constant. It is necessary to include the solvent into the model since its mole fraction is not constant in the layers, see Figure 4. In the extended model, the pressure restricts the mole fractions y_A, y_C of the ions to the physical range $0 \le y_\alpha \le 1$, contrary to classical Poisson-Nernst-Planck model without the pressure correction, where the mole fractions leave the physical range, [4].

Boundary layers. The new electrolyte model allows to resolve the boundary layer. Moreover, by applying the method of formal asymptotic analysis it is now possible to derive a simple reduced model for the bulk region which is supplemented by modified boundary conditions arising from an exploitation of the full model within the boundary layer [4, 8]. The strategy is illustrated in Figure 5 for the variation of a typical variable u near to the actual interface between the electrolyte and a solid metallic electrode.

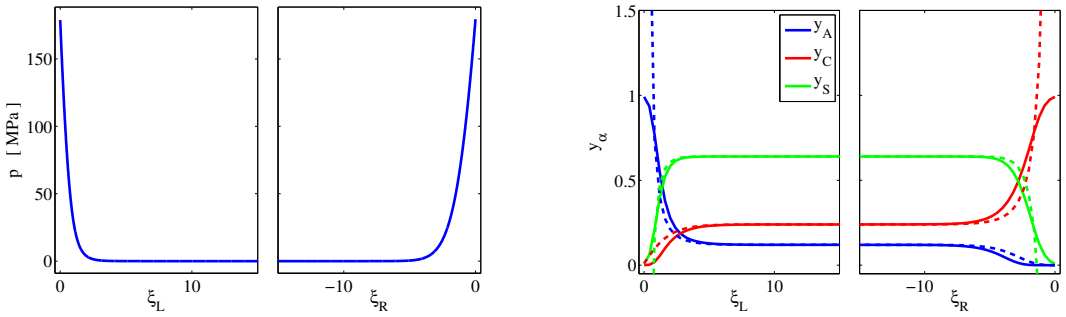

Figure 4: Left: High material pressure in the boundary layers. Right: Comparison of mole fractions computed by the new model (solid) and according to the classical Poisson-Nernst-Planck model (dashed).

The domains of the electrode, the electrolyte and their (actual) interface are indicated by Ω^+, Ω^- and S, respectively. Figure 5_{left} shows the three domains. From left to right we have the electrode (yellow), the interface (black solid line) and the electrolyte (purple). In the bulk domains left and right to the interface we observe the indicated variation of u. Across the interface S the field u has a discontinuity described by the double bracket $[\![u]\!]$. Its determination relies mainly on jump conditions, that are established and exploited in [4, 8]. The parameter λL_0 from above with $0 < \lambda \ll 1$ implies that the variation of u is restricted to a small neighborhood of the interface S. In other words, the parameter λ creates boundary layers left and right to S. This fact is indicated in Figure 5_{middle}. The description of the boundary layers in the limit $\lambda \to 0$ will lead to a new interface I with a new jump that we denote by the triple bracket $[\![\![u]\!]\!]$. On the scale of the limiting case the original interface S with its discontinuity $[\![u]\!]$ is not resolved anymore as it is indicated in Figure 5_{right}.

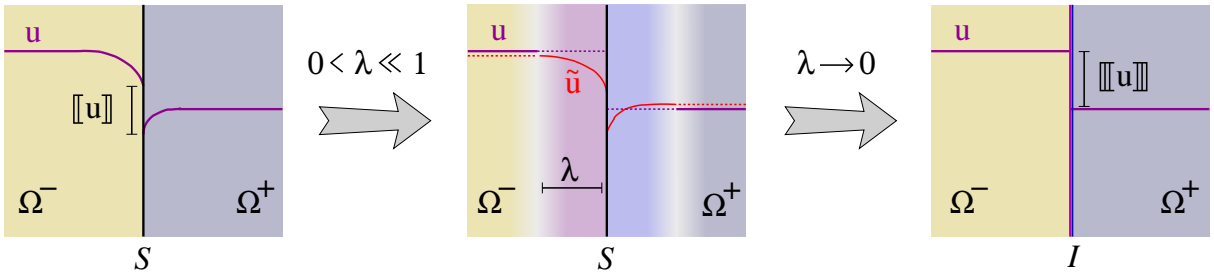

Figure 5: The sharp limit $\lambda \to 0$ of the boundary layer transforms the actual interface S into the interface I with new boundary conditions.

Among the results of the mathematical limit $\lambda \to 0$ we have in the bulk regions $\Omega^\pm$ local charge neutrality, which was postulated in the Nernst-Planck model in the whole domain. Moreover, the limit $\lambda \to 0$ uniquely determines new jump conditions at the interface I, 5_{right}, from the original jump conditions at the interface S, 5_{left}. This result is the essential gain of our approach. In particular, the new jump conditions represent the basis for a rational derivation of so called Butler-Volmer equations describing interfacial electrochemical reactions, [12].

Stern layer revisited. The failure of the Nernst-Planck model to adequately describe the phenomena within the boundary layers has lead many authors to introduce here artificial constructs like *molecular capacitors*. The most relevant version is due to Otto Stern who constructed in 1924 a double layer consisting of a serial connection of two layers.

Stern assumed at the interface of the electrode and the electrolyte an adsorption layer with a linear potential drop toward the electrolyte, Figure 6. Nowadays the adsorption layer is called *Stern layer*. That layer is followed by a so called diffuse layer with exponential decay. The

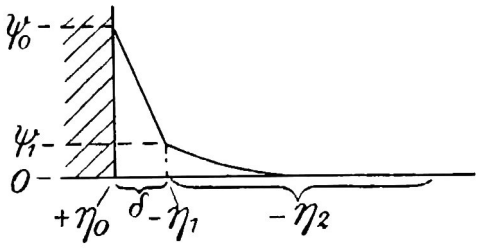

Figure 6: The *Stern-Layer* from the famous 1924 paper of Otto Stern.

ad hoc decomposition of the boundary layer into Stern layer and diffuse layer is necessary in the Poisson-Nernst-Planck setting. This is the reason: If we assume local equilibrium in both layers, which is a good approximation, the Nernst-Planck model implies that the charge density n^{F} becomes a function of the electric potential φ alone and the equation for the potential within the layer is $\lambda^2\Delta\varphi = -n^{\mathrm{F}}(\varphi)$ which is in strong disagreement with experimental data since over 70 years.

In the same context our improved electrolyte model implies that the charge density is a function of the electric potential and of the pressure, [4, 5, 8]. Thus here we have the coupled system

$$\lambda^2\Delta\varphi = -n^{\mathrm{F}}(\varphi, p) \quad \text{and} \quad \nabla p = -n^{\mathrm{F}}(\varphi, p)\nabla\varphi\,. \tag{11}$$

The Figures 7 show the potential and the particle densities within the boundary layer between a metallic electrode and the bulk region of an electrolyte consisting of a 0.5 molar solution of KCl in water according to the new model. The applied voltage between the electrode and the electrolyte is low in the left Figure, and high on the right hand side. In the low voltage regime we observe exclusively a diffuse layer whereas we may identify a decomposition into two different layers in the high voltage regime. Here there is indeed a second layer between the electrode and the diffuse layer as it was proposed by Stern. However, the origin and the properties of our Stern layer differ from Stern's original idea. In the new setting the Stern layer is characterized by a strong decrease of solvent molecules which is accompanied by a saturation of solvated anions. Thus the new model does not rely on an a priori assumed decomposition of the boundary layer. In fact that decomposition is implied by the equations of balance and the corresponding constitutive equations.

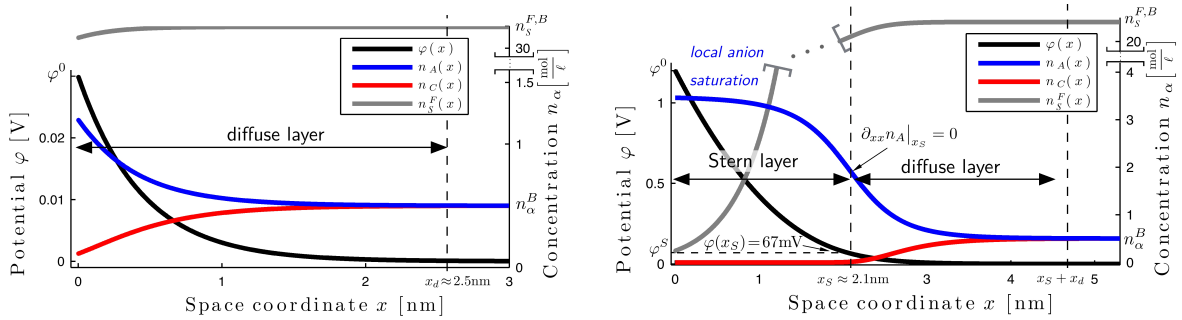

Figure 7: Potential and particle densities within the boundary layer. Left: Low-potential-regime, Right: High-potential-regime, [5]

Solvation. The contribution of the pressure to the mass fluxes J_α increases with the partial molar volume v_α^{R} of the constituents A_α. Since most solvent molecules have a microscopic dipole, there is an additional microscopic electrostatic interaction between solvent and ionic species. This interaction leads to a clustering of κ_α solvent molecules around a central ion of constituent A_α. This is known as solvation effect (cf. Figure 8). The bound solvent molecules

do not participate in the entropic interaction anymore; however, they increase the partial molar volume v_α^{R} of the ionic species. The pressure correction together with the solvation effect yields

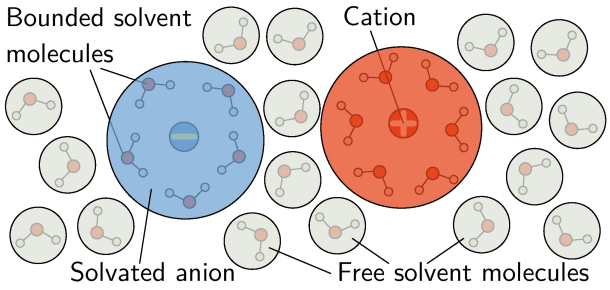

Figure 8: Solvated ions reduce the density of the solvent.

for the first time a physical meaningful boundary layer charge

$$Q_{BL} = -\int_{\Omega_{BL}} n^F \, dx \tag{12}$$

for liquid electrolytes [5]. Figure 9 illustrates the influence of the pressure correction and the solvation effect on the boundary layer charge Q_{BL}. At an applied voltage of 0.25 V the standard Nernst-Planck theory predicts an electric charge of $570\mu\mathrm{C/cm}^2$, while an ideal, incompressible mixture without solvation yields $72\mu\mathrm{C/cm}^2$. Experiments, however, show a charge in the range of $0 - 25\mu\mathrm{C/cm}^2$, which is in good agreement with our new model when a solvation number of $\kappa_\alpha = 15$ is considered.

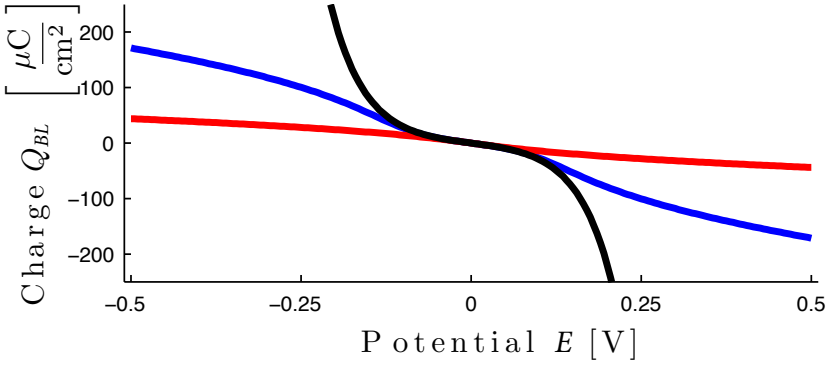

Figure 9: Charge Q_{BL} stored in the double layer as function of the applied potential E for the standard Nernst-Planck model (black), the new Nernst-Planck model without solvation (blue), [4], and with solvation (red), [5, 6].

3.2 Electrode surface model

Modeling the interface between an electrode and some electrolyte is a central aspect for a proper description of batteries and electrochemical systems in general. For this purpose we developed a thermodynamic surface theory that accounts for all aspects occurring on an electrode surface [6, 8, 10]. Similar to the volume phase, the central quantity of surface thermodynamics is the surface free energy density, [9, 6]. All constitutive functions, e.g., the surface chemical potentials $\mu_{s,\alpha}$ and the surface tension γ, are derived from the surface free energy density.

Exemplarily, we studied a metal in contact with a liquid electrolyte. The surface is built by some metal ions M and electrons e, on which electrolytic constituents and their reaction

products, $(A_\alpha)_{\alpha=0,1,\dots,N_s}$, can be present. In contrast to the electrolyte, the metal ions form a lattice with adsorption sites. Not every adsorption site is necessarily occupied, which makes it necessary to introduce the surface vacancies V.

We derived a surface free energy that accounts for the entropical interactions of the adsorbates on the lattice and for the elastic properties of the metallic surface. From this free energy we derived the surface chemical potentials

$$\mu_{s,\alpha} = g_{s,\alpha}(T_s) + \frac{k_B T_s}{m_\alpha} \ln\left(\frac{n_{s,\alpha}}{n_\ell}\right) - \omega_\alpha \frac{k_B T_s}{m_\alpha} \ln\left(\frac{n_{s,V}}{n_\ell}\right), \qquad \text{with } n_\ell = \sum_{\alpha=0}^{N_s} n_{s,\alpha} + n_{s,V}\ , \quad (13)$$

for the adsorbates $(A_\alpha)_{\alpha=0,1,\dots,N_s}$ as well as the surface chemical potentials

$$\mu_{s,M} = g_{s,M}(T_s) + \omega_M \frac{k_B T_s}{m_M} \ln\left(\frac{n_{s,V}}{n_\ell}\right) - \frac{a_M^R}{m_M}(\gamma - \gamma^R) \qquad \text{and} \qquad \mu_{s,e} = const. \quad (14)$$

for the metal ions and the electrons. Here, $n_{s,\alpha}$ denotes the surface mole density and ω_α is the number of adsorption sites of constituent $A_{s,\alpha}$, a_M^R is the partial molar area of the metal surface, and $g_{s,\alpha}(T_s)$ is some reference contribution.

If the adsorption processes are in thermodynamic equilibrium, we have at the surface S

$$\mu_{s,\alpha} = \mu_\alpha\big|_S \qquad \alpha = 0, 1, \dots, N_s, M, e\ , \quad (15)$$

which actually couples the metallic and electrolytic volume phases to the surface. In particular, this leads to an interaction between pressure and surface tension.

Similar to the volume, an adsorbed ion covers $\kappa_{s,\alpha}$ solvent molecules in its solvation shell, which effects the number of adsorption sites ω_α (cf. Figure 10). The solvation shell strongly effects the electric charge which is stored on the surface,

$$Q_S = -\sum_{\alpha=0}^{N_s} z_{s,\alpha} e_0 n_{s,\alpha}, \quad (16)$$

where $z_{s,\alpha} e_0$ is the electric charge of the constituent $A_{s,\alpha}$, $\alpha = 0, \dots, N_s$.

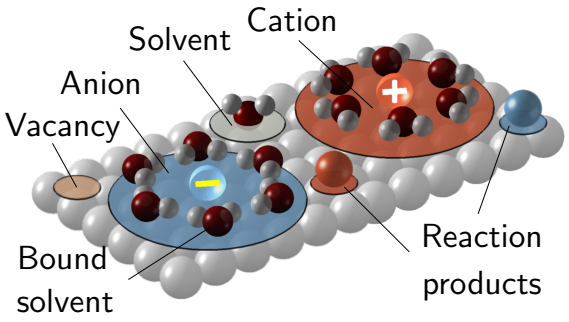

Figure 10: Sketch of the constituents on the surface. Adsorbed ions form a solvation shell.

3.3 Double layer

At an electrode-electrolyte interface, ionic as well as electronic species are accumulated, forming layers of opposite charge. This structure is commonly known as electric double layer, which is a major subject of electrochemistry. Its understanding is of fundamental importance to comprehend the behavior of colloids, dispersion, larger biomolecules, corrosion, electrolysis, electrocatalysis, as well as fuel cells and batteries. Our electrode-electrolyte interface model [6, 8, 12] made substantial contributions to the understanding of the double layer.

In order to validate our theoretical model we consider a planar interface between a metallic single crystal and an electrolytic solution. Precise measurements of such systems are a standard tool for the characterization of new electrodes and electrolytes, as well as of their interaction. One characteristic property of a specific metal-electrolyte interface is the differential capacity C as function of the cell voltage E. Figure 11$_{\text{left}}$ displays the measured capacity of a silver (110) electrode in contact with aqueous $NaClO_4$ solutions of various salt concentrations. In contrast to a plate condenser, where the capacity is a constant, the capacity C of an electric double layer is a highly non-linear function of the voltage E. Thus the capacity is a unique fingerprint of the interface. However, our new model is the first continuum model that is capable to describe the capacity curve over a broad voltage range and for various salt concentrations.

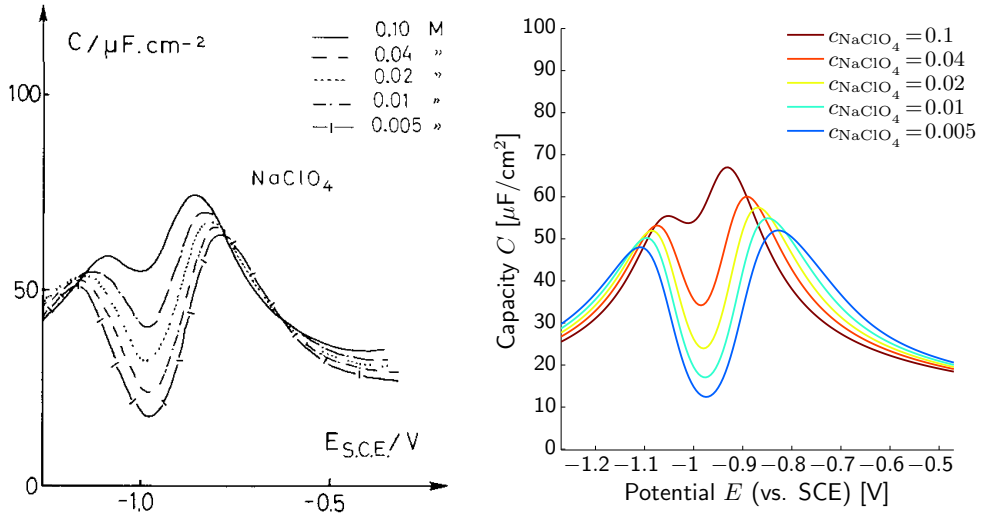

Figure 11: Left: Measured capacity, Fig 2.b from [17], Right: Computed capacity of a Ag(110)|$NaClO_4$(aq) interface

The capacity C is the derivative of the double layer charge Q with respect to the applied potential E, i.e., $C = dQ/dE$. In thermodynamic equilibrium, we obtain Q as a function of the potential drop $\phi_s - \phi^E$ between the metal surface and the electrolyte. Based on balance equations for the electrode charge, we showed that the total charge Q consists of the boundary layer charge Q_{BL} and the surface charge Q_S, i.e., $Q = Q_{BL} + Q_S$. Further, we derived a relationship between the measurable cell potential E and $\phi_s - \phi^E$, namely $E = \phi_s - \phi^E + U^R$, where U^R depends on $\mu_{s,e}$ as well as on the reference electrode. We showed that there exist fundamental relations between the charge contributions Q_{BL} and Q_S and the pressure $p_s = p|_S$ at the surface and the surface tension γ:

$$Q_{BL}(E) = -\text{sgn}(E - U_R)\sqrt{2\varepsilon_r(p_s(E) - p^E)} \qquad \text{and} \qquad Q_S(E) = -\frac{d\gamma}{dE}\,. \tag{17}$$

Many previous and recent approaches to understand the behavior of electrochemical interfaces essentially rely on an a priori conception of the double layer structure. The translation into a mathematical model, however, never has lead to a satisfactory agreement between measured and computed capacity data. In Figure 11$_{\text{right}}$, we display computed capacity curves for a Ag(110)—$NaClO_4$(aq) interface. We find a remarkable agreement between the experimental data and our new model, both in the potential range of 1V and the salt concentration range $c = [0.005 - 0.1]$M.

After validating our model on measured capacity data, we can analyze the structure of the space charge layers that are predicted by the model. We find the formation of several layers in front of the metal surface, which can be reinterpreted in terms of the classical conception of the double layer; see Figure 12. However, we find also some crucial deviations from the doctrine

of the classical literature, e.g., emphthe Stern layer width is not constant, but grows with the applied potential [5, 6].

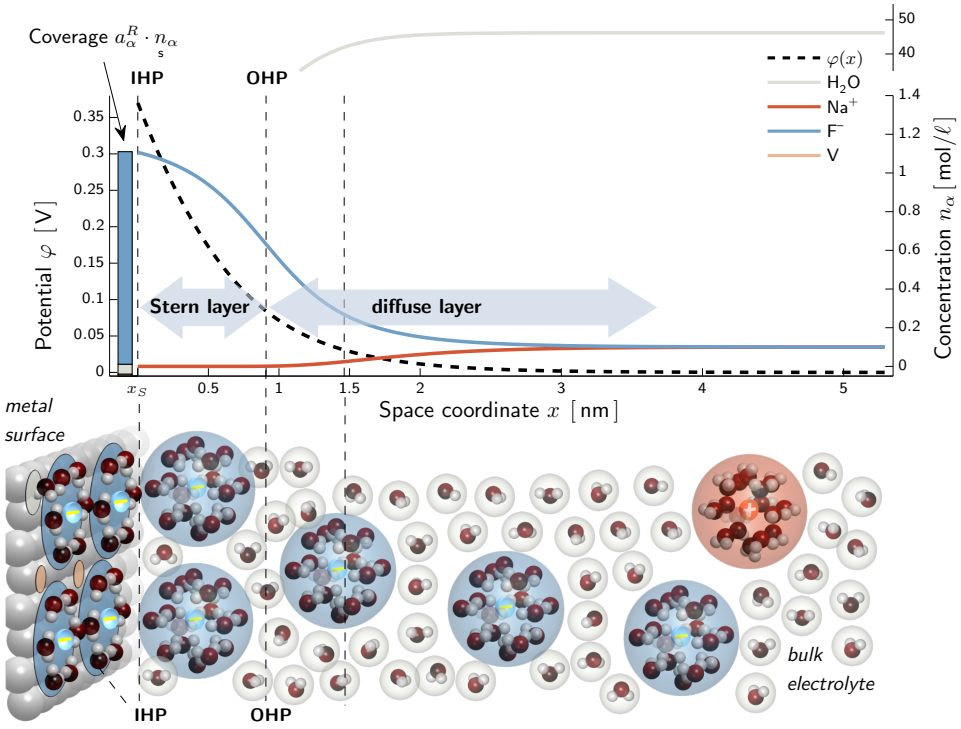

Figure 12: Computed charge structure and potential at the metal-electrolyte interface with a sketch of our reinterpretation of the double layer structure.

3.4 Electron transfer reactions

Energy conversion in batteries requires electrochemical surface reactions that take place at the contact between electrodes and the electrolyte. In particular the understanding and mathematical description of electron transfer reaction has always been a central question in electrochemistry.

For simple electrochemical systems such as a metal in contact with a liquid electrolyte, it is observed that the surface reaction rate R, or equivalently the electric current density j^e, is related to a potential difference at the interface, the surface overpotential η_S. The most simple relation of this kind is the empirical Tafel-equation

$$\eta_S = a + b \, \log(j^e), \tag{18}$$

where the coefficient a and b are phenomenological coefficients. A more general relation that accounts for simultaneous anodic (oxidation) reaction and cathodic (reduction) reaction on the same electrode surface is the Butler-Volmer equation. It reads

$$R = R^0_{\mathcal{A}} \, \exp\left(\frac{\alpha_{\mathcal{A}} \, e_0}{kT}\eta_S\right) - R^0_{\mathcal{C}} \, \exp\left(-\frac{\alpha_{\mathcal{C}} \, e_0}{kT}\eta_S\right). \tag{19}$$

Herein $R^0_{\mathcal{A}/\mathcal{C}}$ are called anodic and cathodic exchange rates, respectively, which can be general functions of the temperature T and the concentration of the different chemical species. The transfer coefficients $\alpha_{\mathcal{A}}$ and $\alpha_{\mathcal{C}}$ are considered as phenomenological coefficients.

Originally, the derivation of the Butler-Volmer equation is based on kinetic theory and still (19) is lacking a foundation in non-equilibrium thermodynamics. For the derivation of (19) in the context of non-equilibrium thermodynamics it is important to bear in mind that

1. The definition of η_S is not evident from modeling based on non-equilibrium thermodynamics where the set of thermodynamic variables contains the electric field $\boldsymbol{E} = -\nabla\varphi$ but not a potential φ itself or some potential difference.

2. Further the interfacial Maxwell equations require that the electric potential φ is continuous at an interface. Therefore no natural potential difference exists, which can be used to define an overpotential.

3. The generality of $R^0_{\mathcal{A}/\mathcal{C}}$ is restricted by the 2$^{\mathrm{nd}}$ law of thermodynamics. In consequence, the forward and backward reaction can not be modeled independently.

In the context of our electrolyte-electrode interface model, where the diffuse charge layers are spatialy resolved, the constitutive laws for the interfacial reaction rates are not of Butler-Volmer type [8, 13]. Under the assumption of appropriate scaling relations, the double layer can asymptotically be considered in equilibrium and we are able to derive a reduced model. The reduced model is discribed in Section 3.1 and the asymptotic analysis of the charge layers is illustrated in Figure 5. Within this reduced model, we are able to define an overpotential and to recover relations of Butler-Volmer type for the interfacial reaction rates [8, 12]. For simplicity we consider a single surface reaction of the form

$$a_0 A_0 + \cdots + a_N A_N \rightleftharpoons b_0 A_0 + \cdots + b_N A_N \tag{20}$$

where each constituent is at least defined in one of the bulk phases. In that case we derive a general Butler-Volmer equation of the form

$$R = R^0_f \, \exp\Big(- \frac{\alpha_f \, e_0}{kT} \eta_S \Big) \; - R^0_b \, \exp\Big(+ \frac{\alpha_b \, e_0}{kT} \eta_S \Big) \, . \tag{21}$$

The overpotential as well as the coefficients are defined as

$$\eta_S = [\![\varphi - \bar{\varphi}]\!] \, , \tag{22}$$

$$\alpha_f = \beta A \sum_{\alpha \in M^+} \gamma_\alpha z_\alpha \, , \tag{23}$$

$$\alpha_b = (1-\beta) A \sum_{\alpha \in \mathcal{M}^+} \gamma_\alpha z_\alpha \, , \tag{24}$$

$$R^0_f = R_0 \, \exp\left(\quad - \underset{s}{\beta} \frac{A}{kT} \sum_{\alpha \in \mathcal{M}} \gamma_\alpha m_\alpha \big(\mu_\alpha - \bar{\mu}_\alpha\big)\big|^{\pm}_I \right) \, , \tag{25}$$

$$R^0_b = R_0 \, \exp\left((1-\beta) \frac{A}{kT} \sum_{\alpha \in \mathcal{M}} \gamma_\alpha m_\alpha \big(\mu_\alpha - \bar{\mu}_\alpha\big)\big|^{\pm}_I \right) \, . \tag{26}$$

The potential difference η_S then describes the deviation of the actual potential difference $\varphi|^+_I - \varphi|^-_I$ from the equilibrium voltage $\bar{\varphi}|^+_I - \bar{\varphi}|^-_I$ of the bulk phases. This result is in accordance with usual definitions in electrochemistry.

The general Butler-Volmer equation (21) does not depend on a specific experimental setup, rather the functions are expressed in terms of the chemical potentials instead of concentrations or particle densities.

Thus the application of the new Butler-Volmer equation to different specific application scenarios is directly possible. We have considered electron transfer reactions at metal electrodes, adsorption processes and paricularly the intercalation process in lithium-iron-phosphate electrodes.

Our general Butler-Volmer equation can only be valid as long as the assumptions of the underlying reduced bulk model hold. Let us discuss this in detail. First of all, the reduced bulk model requires that “the Debye length is small”. That means, we choose a characteristic

length scale L^R for the electrochemical system under consideration, such that the overall size of the system is comparable to L^R and the curvature of surfaces is less than $1/L^R$. Then the Debye length, which controls the width of boundary layers, has to be smaller than L^R by some orders of magnitude. In consequence, the Butler-Volmer equation (21) can not be applied in the context of nano-systems. Second, the derivation of the reduced bulk model is based on quasi-equilibrium of the boundary layer. For this, it is necessary that relaxation times of the layer are small compared to the macroscopic experimental timescales. In [8], a macroscopic time scale of $t^R = 10s$ was used.

This certainly rules out the application of (21) to processes where excitations due to short pulses or high frequencies are applied. In these cases our complete electrode/electrolyt model, where the charge layers are spatially resolved, has to be used.

3.5 Many-particle electrode model

$LiFePO_4$ (LFP) is a promising material for the lithium-ion battery market. A LFP electrode consists of many LFP particles of nanometer size on a metallic substrate. The particle ensemble exists as a size distribution in the range of 25 – 500 nm. During the discharging process of the battery, lithium atoms are reversibly stored on interstitial lattice sites of the iron phosphate lattices. This storage process is accompanied by a phase transition from a lithium-poor to a lithium-rich phase. In 2010, a new model was proposed at WIAS that demonstrated that the phase transition occurs within the many-particle system and not within the individual storage particles on the time scale of charging/discharging [2, 3]. The many-particle effect is the crucial process that controls the behavior of the LFP electrode. Recently, this new idea was experimentally confirmed by W.C. Chueh et al. [14, 15] on the characteristic time scale of battery charging/discharging.

The LFP particles are not all of equal size, but follow a particle size distribution function; see Figure 3. In order to investigate the effect of various distribution functions, e.g., arising from different synthesis and production methods, we developed a new model that describes the charging process by a system of stochastic differential equations. For each of the N_P LFP particles $(P^i)_{i=1,\dots,N_P}$ there is a stochastic differential equation

$$dy^i = \frac{1}{\tau^i}\big(\mu_{s,Li} - \mu^i_{Li}\big)dt + \frac{\sqrt{2}\nu^i}{\sqrt{\tau^i}}dW^i \qquad \text{with} \qquad \tau^i = \tau_0\tfrac{V^i}{A^i} \quad \text{and} \quad \nu^i = \nu_0\tfrac{1}{\sqrt{V^i}}\,, \tag{27}$$

where $y^i = n^i_{Li}/n_{FePO_4}$ denotes the lithium mole fraction, V^i the volume, and A^i the surface area of particle P^i. Since LFP is a phase-separating material, μ_{Li} represents the non-monotone chemical potential of intercalated lithium. Micro fluctuations on the particle surface are modeled by a Wiener process W^i, where ν_0 controls the strength of the fluctuations. The rate of the intercalation process is controlled by $\tau_0 > 0$, where $\tau_0 \to 0$ corresponds to fast intercalation, while $\tau \to +\infty$ corresponds to slow intercalation.

Due to the assumed fast surface diffusion, the surface chemical potential $\mu_{s,Li}$ is the same for all particles. It is controlled by a relation between the lithium mole fractions y^i and the electric current I,

$$Idt = -e_0 n_{FePO_4} \sum_{i=1}^{N_P} V^i dy^i\,. \tag{28}$$

Typically, the distance between the electrodes of a battery is smaller than $100\,\mu$m. Due to the high mobilities of the species in the electrode and the electrolyte, the time-depending behavior of the battery is exclusively controlled by surface phenomena. Based on our general electrode-electrolyte interface theory [9, 8, 12], we are able to derive a relation for the voltage between the many-particle electrode and metallic lithium,

$$U = U_0 - \tfrac{1}{e_0}\mu_{s,Li} + (R_{ad} + R_{re})I\,. \tag{29}$$

Here, R_{ad} and R_{re} are resistances, which take into account the lithium adsorption from the electrolyte to the electrode surface and the electron transfer reaction $Li^+ + e^- \leftrightharpoons Li$ at the surface.

The particle size distribution has a large impact on the dynamics of the many particle electrode. Figure 13 shows simulations in the fast charging/discharging regime for two electrodes with the same total particle volume $V = \sum_i V^i$ but with different particle size distributions. In the case of identical particle sizes and fast charging all particles behave identical and the surface chemical potential $\mu_{s,Li}$ follows the non-monotone chemical potential μ_{Li} of a single particle. In particular no phase transition occurs in the particle ensemble. However, if the particle size distribution is given according to Figure 3, the particles of the electrode behave differently and a phase transition in the ensemble takes place. This behavior in the fast charging/discharging regime is in accordance with experimental results [15].

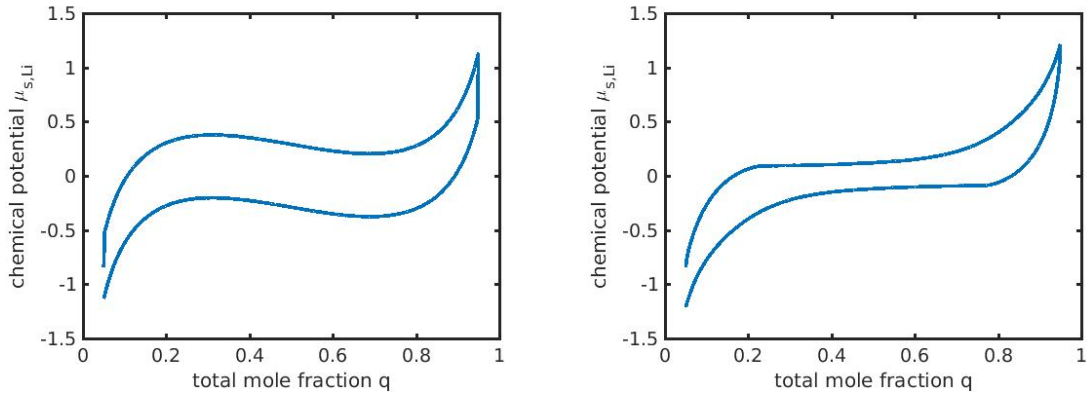

Figure 13: Charging/discharging hysteresis for different particle size distributions in the fast charging/discharging regime. Left: all particles are identical, right: particle size distribution according to Figure 3.

The new model is capable to simulate the voltage-capacity diagram for a LFP electrode shown in Figure 14 with a typical particle size distribution as shown in Figure 3. The simulation shows all features of the experimental data given in Figure 1_{right}, where only two parameters τ_0 and ν_0 have to be adjusted.

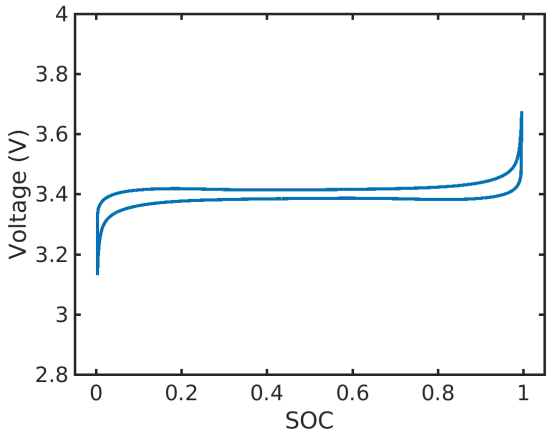

Figure 14: Computed voltage-capacity diagram for a LFP many-particle electrode with 7000 particles.

References

[1] W. Dreyer, J. Jamnik, C. Guhlke, R. Huth, J. Moškon and M. Gaberšček, The thermodynamic origin of hysteresis in insertion batteries, Nature Materials, **9** (2010), pp. 448–453.

[2] W. Dreyer, C. Guhlke, R. Huth, The behavior of a many particle cathode in a lithium-ion battery, Physica D, **240** (2010), pp. 1008–1019.

[3] W. Dreyer, C. Guhlke, M. Herrmann, Hysteresis and phase transition in many-particle storage systems, Continuum Mechanics and Thermodynamics, **23** (2011), pp. 211–231.

[4] W. Dreyer, C. Guhlke, R. Müller, Overcoming the shortcomings of the Nernst-Planck model, Physical Chemistry Chemical Physics , **15**(19) (2013), pp. 7075–7086.

[5] W. Dreyer, C. Guhlke, M. Landstorfer, A mixture theory of electrolytes containing solvation effects, Electrochemistry Communications, **43** (2014), pp. 75–78.

[6] W. Dreyer, C. Guhlke, M. Landstorfer, Theory and structure of the metal/electrolyte interface incorporating adsorption and solvation effects, WIAS Preprint no. 2058, (2014), submitted.

[7] W. Dreyer, P. Friz, P. Gajewski, C. Guhlke, M. Maurelli, Stochastic modeling and analysis of many-particle electrodes, WIAS Preprint no. 2202, (2015).

[8] W. Dreyer, C. Guhlke, R. Müller, Modeling of electrochemical double layers in thermodynamic non-equilibrium, Physical Chemistry Chemical Physics, **17**(40) (2015), pp. 27176–27194.

[9] C. Guhlke, Theorie der elektrochemischen Grenzfläche, Doctoral thesis, TU Berlin (2015).

[10] W. Dreyer, C. Guhlke, M. Landstorfer, R. Müller, New insights on the interfacial tension of electrochemical interfaces and the Lippmann equation, WIAS Preprint no. 2201, (2015).

[11] W. Dreyer, C. Guhlke, Sharp limit of the viscous Cahn–Hilliard equation and thermodynamic consistency, Continuum Mechanics and Thermodynamics, (2015), doi:10.1007/s00161-015-0434-5.

[12] W. Dreyer, C. Guhlke, R. Müller, A new perspective on the electron transfer: Recovering the Butler-Volmer equation in non-equilibrium thermodynamics, WIAS Preprint no. 2204, (2015).

[13] W. Dreyer, D. Bothe, Continuum thermodynamics of chemically reacting fluid mixtures, Acta Mechanica, **229**(6) (2015), pp. 1757–1805.

[14] W.C. Chueh, F. El Gabaly, J.D. Sugar, N.C. Bartelt, A.H. McDaniel, K.R. Fenton, K.R. Zavadil, T. Tyliszczak, W. Lai, K.F. McCarty, Intercalation Pathway in Many-Particle LiFePO4 Electrode Revealed by Nanoscale State-of-Charge Mapping, Nano Letters, **13**(3) (2013), pp. 866–872.

[15] Y. Li, S. Meyer, J. Lim, S.C. Lee, W.E. Gent, S. Marchesini, H. Krishnan, T. Tyliszczak, D. Shapiro, A.L.D. Kilcoyne, W.C. Chueh, Effects of Particle Size, Electronic Connectivity, and Incoherent Nanoscale Domains on the Sequence of Lithiation in LiFePO4 Porous Electrodes, Advanced Materials, **27**(42) (2015), pp. 6591–6597.

[16] M. Safaria, C. Delacourta, Mathematical Modeling of Lithium Iron Phosphate Electrode: Galvanostatic Charge/Discharge and Path Dependence, Journal of The Electrochemical Society,**158**(2) (2011), pp. A63–A73.

[17] G. Valette, Double layer on silver single-crystal electrodes in contact with electrolytes having anions which present a slight specific adsorption: Part I. The (110) face, Journal of Electroanalytical Chemistry and Interfacial Electrochemistry, **122** (1981), pp. 285–297.